COBEM 2023 27TH INTERNATIONAL CONGRESS OF MECHANICAL ENGENEERING

ABCM Brazilian Society of Mechanical Sciences and Engineering
27th ABCM International Congress of Mechanical Engineering
December 04-08, 2023, Florianópolis-SC, Brazil

COB-2023-1568
STRUCTURAL OPTIMIZATION OF THE FUSELAGE HULL OF A COMPOSITE GROUND EFFECT VEHICLE

Felipe Araújo Bortolete
Lucas Souza
Aircraft Design Department, Aeronautics Institute of Technology, São José dos Campos, Brazil, and Barco Voador Engenharia e Desenvolvimento LTDA, Manaus, Amazonas
felipe.bortolete@ga.ita.br
lucas.guimaraes@ga.ita.br

Manuel Alejandro Rodriguez Diaz
Barco Voador Engenharia e Desenvolvimento LTDA, Manaus, Amazonas
manuel.rodriguez@aeroriver.com.br

Ney Rafael Secco
Aircraft Design Department, Aeronautics Institute of Technology, São José dos Campos, Brazil
ney@ita.br

Abstract. *With great economic potential, the Amazon always generates major logistical problems, mainly caused by its extensive territory linked to its huge lack of infrastructure. In a context where solutions designed to meet the specificities of each region make more and more sense, the use of wing ground effect vehicles (WIG) presents characteristics capable of helping to solve several logistical bottlenecks that lived in the region. Historically, this type of vehicle has mostly been used for operating in closed seas, which is why operating in Amazonian rivers has its particularities, a critical point being the constant risk of impact with a piece of wood during takeoff and landing. Thus, the use of a hull consisting of a structure of sandwich panels combined with composite materials would give this hull excellent robustness. Moreover, this type of material has the advantage of being lightweight, mechanically resistant and durable, thermally insulating and long-lasting. With this background, the present work aims to perform a structural optimization of the hull of a ground effect vehicle made of composite materials, manufactured by methods commonly used in the marine industry, in order to evaluate whether these methods can meet the requirements of this type of vehicle. For this purpose, a literature review was first conducted to identify the design rules. Then, a MATLAB code was created to estimate the main loads due to the operation of the vehicle. The format of the hull was determined and the design variables used were the thickness of the painels, stiffeners and frames that form the structure of the hull. The results show a structural layout with a high resistance index, capable of withstanding the loads to which the vehicle will be subjected and demonstrating an excellent relationship between structural weight and resistance.*

Keywords: *Structural Optimization, WIG, Ground Effect.*

1. INTRODUCTION

The Amazon region has great economic potential, but it also always presents major logistical problems, mainly due to the extent of the territory combined with the enormous lack of infrastructure. The Legal Amazon covers an area of more than 5.2 million km^2 - 61% of Brazil's territory - of which 5.1 million km^2 is land and 96,000 km^2 is water. The region represents a strategic point of the national territory, containing 20% of the world's available freshwater and more than 30% of forest reserves (Coelho, 2010). A study conducted by Costanza *et al.* (2014) estimates the potential for wealth creation in the Amazon at about 7 trillion reais per year. Unfortunately, all these areas and the economic potential are not being properly exploited. This is mainly due to this are the logistical factors, which become an insurmountable obstacle to development in such a vast region with so many peculiarities.

On the other hand, technological development has simplified the development of solutions that were once considered complex technical solutions. This allows the development of innovative solutions and promotes the emergence of new markets. As an example, we can mention the creation of companies for the development of electric vertical take-off and landing vehicles (eVTOL), which would have been unthinkable 20 years ago.

In this scenario, the use of a ground effect vehicle (WIG) designed for use in Amazon rivers makes a lot of sense and offers great potential for economic gain. In the past, the use of this type of vehicle did not catch on worldwide because there were some technical problems in its operation that are now easier to circumvent thanks to new technologies. Another concern that is becoming increasingly important is the delicate balance of the world's ecosystem and the fact that carbon dioxide emissions caused by transportation are upsetting this ecosystem (Wiriadidjaja *et al.*, 2018). Therefore, it makes a lot of sense to think about a vehicle that offers higher energy efficiency as a transportation solution for a region that is so important for the preservation of this ecosystem.

To operate in the Amazon, a ground effect vehicle must have a lightweight and very reinforced hull, because one of the biggest problems for amphibious aircraft operating in the Amazon is debris in the river, because pieces of trees on the surface of the water are not uncommon, which can cause accidents during takeoffs and landings. Therefore, the use of a hull consisting of a structure made of sandwich panels combined with composite materials would give this hull excellent robustness to impact loads. In addition, this type of material has the advantage of being lightweight, mechanically and corrosion resistant, well thermally insulating and durable.

In this context, the present work aims to carry out a structural optimization of the hull of a ground effect vehicle made of composite material, in order to obtain a lightweight structure with greater resistance to the various impact loads to which the vehicle will be subjected throughout.

2. GROUND EFFECT VEHICLE

The term ground effect (GE) is an aerodynamic phenomenon that occurs when the wing of an aircraft is very close to a surface. This phenomenon is characterized by an increase in the lift-to-drag ratio (L/D) of a wing at altitudes lower than the chord length of the wing, and it becomes more pronounced at altitudes below 25% of the chord and is classified as extreme ground effect (Rozhdestvensky, 2000). As the wing approaches the water surface, the free airflow below the wing can no longer expand, further increasing static pressure and hence lift (Halloran and O'Meara, 1999). To take full advantage of this energy efficiency zone, a WIG must spend most of its travel in this altitude range.

The idea of the ground effect vehicle idea is not new. From the 1960s to the 1980s, the ground effect vehicle concept was introduced (Fig. 1), mainly for military purposes and later for commercial concepts (Papadopoulos *et al.*, 2022). den Breejen (2018) characterizes ground effect vehicles (WIG) as vehicles that use ground effect to operate at low flight altitudes, at altitudes from 0 to 5 meters above water. The forward velocity is used to produce dynamic lift. In this way, drag, which depends on lift, is reduced. It can be said that the closer the vehicle operates to the surface, the more energy efficient it becomes, due to that the power required to fly the vehicle is considerably lesser than a ship that might possibly be used in its case. The main reason for the interest in this type of vehicle is that they are more energy efficient than ships and airplanes in the speed range between 150-350 km/h (Yun *et al.*, 2010).

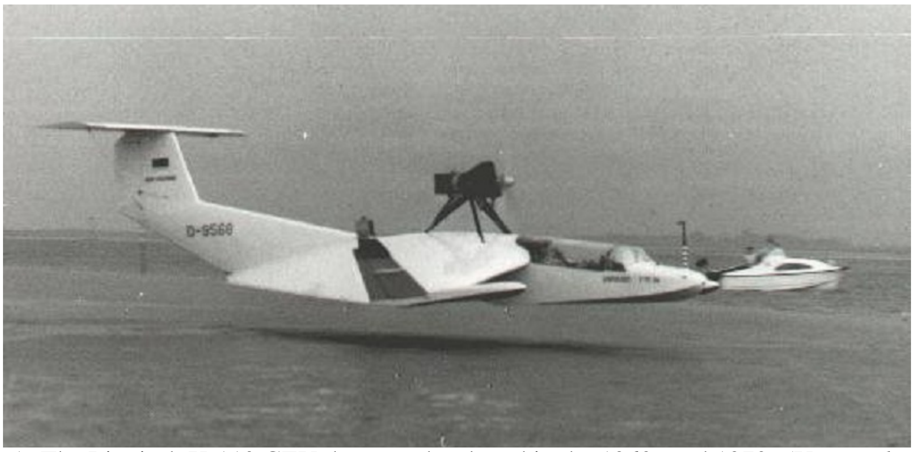

Figure 1: The Lippisch X-113 GEV that was developed in the 1960s and 1970s (Yun *et al.*, 2010).

Nebylov (2001) distinguishes four main advantages of WIG vehicles, as shown below:

- No need for airports;
- Increased flight safety due to low altitude and the ability to land on water;
- Ability to carry a larger payload with smaller main dimensions
- Passenger comfort level can be close to that of a conventional ship.

Until 2002, WIG vehicles did not meet any standard set by the International Maritime Organization (IMO) and the International Civil Aviation Organization (ICAO). Until December 2002, the Maritime Safety Committee approved interim guidelines for WIG vessels (MSC/Circ.1054 and Corr.1) to be used with appropriate engineering analysis, design, and developmental testing to achieve an inherently safe vessel, and agreed that their relevance and suitability should be evaluated as experience is gained with their use. In 2018, the Maritime Safety Committee adopted guidelines for wing-in-ground craft, in IMO Regulation MSC/Circ.1592 (GUIDELINES FOR WING-IN GROUND CRAFT). Since then, this has been the current regulation for this type of vehicle.

WIGs are technically flying boats, as they are equipped with a hull that allows them to takeoff and land from the water. Therefore, their hull design has its peculiarities, as it differs from a convection vessel due to the vertical accelerations, while at the same time it does not have to meet the safety level of a seaplane. The abrupt end of the development of WIG in the late 1980s has resulted in little research being available, as none of these concepts ever reached mass production and this fact continues to be a design challenge today (Papadopoulos *et al.*, 2022). For this reason, this article addresses both high-speed vehicle hull design and seaplane hull design. The goal is to develop a new methodology that integrates both previous methods while being specific to ground effect vehicle hull design.

3. HULL DESIGN

One of the major disadvantages of WIGs is the high power required for launch and the high structural overhead associated with the hull hitting the waves during launch, which is called slamming and is the critical design parameter for the hull (Halloran and O'Meara, 1999). Therefore, when designing a ground effect vehicle, the two most important requirements are lightness and resistance. Lightness is necessary to ensure the performance of the vehicle, and resistance is important to ensure that the vehicle can withstand the loads during launch.

Generally, the materials used in the manufacture of high-speed boat hulls are: naval steel, aluminum, and composites. Naval steel, although a proven construction method, has lower corrosion resistance and a high specific mass, resulting in a high weight of the hull. Aluminum, on the other hand, has low specific mass, good mechanical properties and high corrosion resistance, but its use imposes certain limits on the geometry of the hull. Composites, on the other hand, combine high mechanical properties and corrosion resistance with low weight and allow greater control over the shape of the hull with excellent surface finishes (Amaral, 2016). Based on these characteristics, it is concluded that the use of composite materials is the most suitable solution for the production of a WIG hull to be used in the Amazon region, since this type of material offers good mechanical properties as well as high corrosion resistance. the problem of corrosion is another major issue with metal alloy vehicles used in this region.

The hull structure of amphibious aircraft must be designed to withstand the load during landing or takeoff without damage (Kamarul *et al.*, 2017). For this purpose, the structure of the hull consists of planking supported by sections distributed longitudinally and transversely across the hull (Cardoso, 1994). In this way, the structural project includes the determination of the thickness of the panels or laminates and the dimensions and positioning of the longitudinal stiffeners and transverse web frame that make up the hull. These structural elements are dimensioned to withstand static and dynamic pressure, and the project must be carried out in accordance with the standard of a classification society. Figure 9a shows the typical structural arrangement of a high-speed vessel. In composite structures, the stiffeners are laminated to the hull (Amaral, 2016).

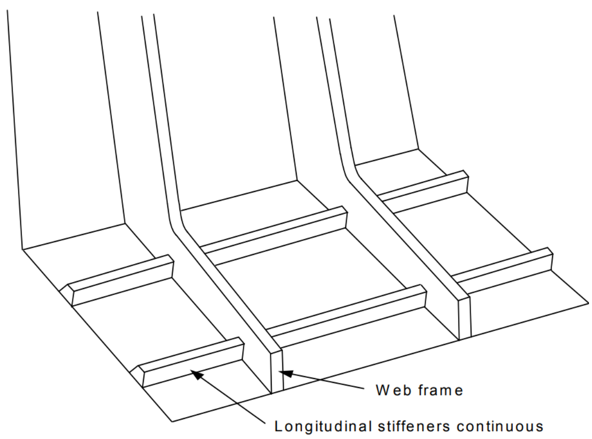

Figure 2: Typical stiffener and frame structure (DNV, 2012).

4. COMPOSITE MATERIALS

The word composite un the terme *composite material* signifies that two or more material are combined on a macroscopic scale to form a useful third material (Jones, 1998). Fiber-reinforced composite materials, for example, contain high strength and high modulus fibers in a matrix material. In these composites, fibers are the principal load-carrying members, and the matrix material keeps the fibers together, acts as a load-transfer medium between fibers, and protects fibers from being exposed to the environment (Reddy, 2003).

Composite materials are classified as anisotropic, meaning that material properties can vary in both position and direction. Therefore, the design and analysis of composite structures is much more complex than for metals (Budynas and Nisbeth, 2016). Another major difference between composites and isotropic materials lies in their failure criteria. This is because to ensure the safety of an anisotropic material, a larger number of design variables must be evaluated during structural analysis, such as lamina thickness, order, and fiber orientation angle.For the present work, it was decided to use the Tsail-Hill failure criterion (Tsai and Wu, 1971). This theory is based on the maximum deformation energy criterion for isotropic materials or the Von Mises criterion, with modifications for anisotropic materials. The deformation energy is one of the parts of the deformation energy of a body, since it consists of two parts, one related to the change in volume of the body, called the expansion energy, and the second related to the change in shape, called the deformation energy (Silva and Cavalcante, 2016). Thus, it is assumed that material failure occurs only when the deformation energy is greater than the material failure deformation energy given by :

$$\frac{\sigma_x'^2}{X^2} - \frac{\sigma_x'\sigma_y'}{X^2} + \frac{\sigma_y'^2}{Y^2} + \frac{\tau_{xy}'^2}{S^2} = 1 \qquad (1)$$

Where σ_x, σ_y are normal stress in the longitudinal and transverse axes of the fibers, and τ_{xy} is shear stress, and X is longitudinal tensile strength in the x direction, and Y is transverse tensile strength in the y direction, and S is Shear strength in the x-y plane.

4.1 Manufacturing Processes

With the aim of testing the manufacturing processes used in the marine industry for this type of application, a manufacturing process commonly used for the construction of fiberglass boat hulls was selected. This process is vacuum infusion lamination: a method that guarantees a better quality of the part, since excess resin, volatiles and air bubbles that could affect the mechanical properties are removed more efficiently (Neto and Pardini, 2006). The process is determined by the preparation of the mold, the placement of the fabric and the core on the mold, the covering of the mold with a flexible bag and the application of a vacuum. In vacuum lamination, the resin is applied to the fabric or cloths before covering the mold. In infusion, the resin is distributed throughout the part when the vacuum is applied. In both processes, the excess resin is removed by the vacuum, ensuring a volume content of up to 50% (Badini, 2013).

The bottom is made of single-layer laminate. This means that it consists exclusively of layers of woven and loose glass fibers held together by epoxy resin.The structural grid is composed by frames and stiffeners.The sides are made of a sandwich structure. It is a core of polymer foam with two thin glass fiber laminates on each side. The foam core reduces weight while still has shear resistant. This construction technique is only used on the sides, as this part of the vessel does not suffer as much from hydrodynamic forces. This structural layout is based on the work of Rayes and Tancredi (2013).

4.2 Material Properties

For the design of the structural parts of the hull, the material properties from Tab. 1 were used.

Table 1: Material properties used in the hull (Rayes and Tancredi, 2013).

	Fiberglass	**Epoxy resin**
Rupture Stress (MPa)	122.5	-
Density (kg/m³)	2600	1300
Percentage in mass (m)	50%	50%
Poisson's coefficient (t)	0.3	-

5. METHODOLOGY

Figure 3 shows a flowchart of the operation of the platform. The process begins with the dark blue ellipse representing the optimization solver that provides the input data for the blue square, the code responsible for calculating the stiffness and structural mass of the hull. Following the red ellipse, a check is made to see if the fuselage can withstand the estimated takeoff and landing loads; if not, that individual is eliminated. In the end, the optimizer looks for the individual with the lowest mass that can withstand the calculated loads.

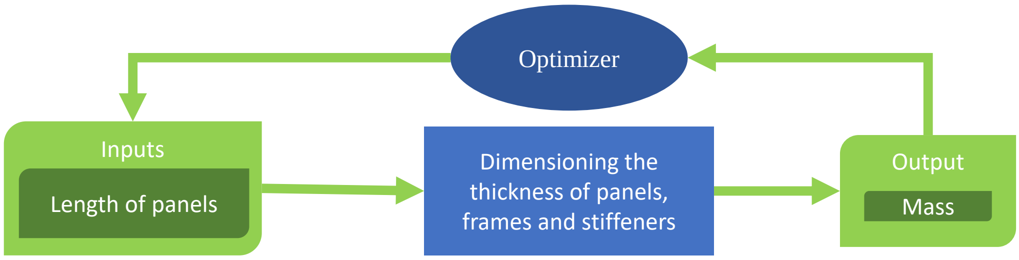

Figure 3: Optimization workflow.

5.1 Optimizer

The MATLAB function gamultiobj, a multi-objective genetic algorithm function, is used to guide optimization because of its flexibility in dealing with complex and multidisciplinary problems. The function was configured to generate 100 generations with 50 individuals (Mathworks, 2018).

5.2 Hull Characteristics

The geometric characteristics of the hull under study were determined prior to this work. Table 2 shows the main characteristics of the hull used. This geometry was designed with the aim of ensuring good stability and not generating a large hydrodynamic drag to reduce the power required for takeoff.

Table 2: Dimensions and characteristics of the hull studied.

Hull Characteristics	**Symbol**	**Value**
Design Length (m)	L_{pp}	7,78
Design Beam (m)	B	2,26
Design Draft (m)	T	0,45
Displacement (t)	Δ	3
Block Coefficient	C_B	0,361

5.3 Technical design rules for hull sizing

The blue square in the flowchart in Fig. 3represents the part of the code responsible for calculating the loads and sizing the thickness of panels, frames and stiffeners. For the structural design of the hull, the “DNV Rules for the Classification of High-Speed, Light and Surface Naval Vessels” were used, specifically the chapters on design loads (Part 3, Chapter 1) and structural design (Part 3, Chapter 4). The methodology used was to apply the formulation proposed by (DNV, 2012) to calculate the loads along the length of the hull and to determine the dimensions of the structural elements. This methodology was based on the work of citetrayes.

5.3.1 Vertical acceleration

The analysis of design loads begins by determining the vertical acceleration experienced by the hull along its length. This vertical acceleration results from the interaction of the vessel with the ocean waves, which leads to an instantaneous upward motion. This force resulting from the impact is commonly referred to as "slamming pressure" in the guidelines.

In the regulations, specifically in Part 3, Chapter 1, Section 2, there is a formula called B201. This formula is used to determine the vertical acceleration at the center of gravity:

$$a_{cg} = \frac{V}{\sqrt{L}} \frac{3.2}{L^{0.76}} f_g g_0 \tag{2}$$

Where a_{cg} is the vertical acceleration at center of gravity in m/s², V is the maximum operation speed in knots, L is the length at waterline in meters, f_g is an acceleration factor depending on the type of vessel, being 1 for passenger vessels, g_0 is the acceleration of gravity in m/s². After calculating the vertical acceleration at the center of gravity, equation B202 of the rule is used to calculate the loads along the length of the hull:

$$a_v = k_v a_{cg} \tag{3}$$

Where a_{cg} is the vertical acceleration along the length of the hull and k_v iis a longitudinal distribution factor given by the rules.

Using the acceleration obtained in Eq. (2), it is calculated through Eq. (3) the vertical accelerations along the hull, Fig. Fig. 4 . A gravity of 9.81 m/s², a hull length of 7.78 m and, due to the nature of the vehicle, a speed of 81 knots (150 km/h) were considered for this calculation for safety reasons, even though the vehicle does not come into contact with the water at this speed.

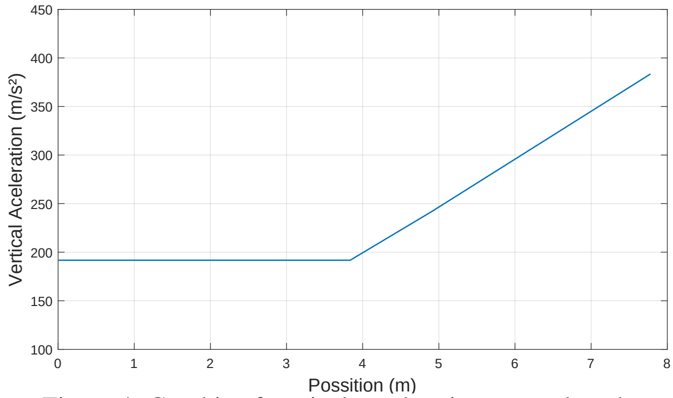

Figure 4: Graphic of vertical acceleration versus length.

5.3.2 Design pressures

In Part 3, Chapter 1, Section 3 of the technical rules, no loads on the hull girder are to be considered in vessels with an L/D of less than 12 and a length of less than 50 meters. Thus, the design pressure for the bottom and side is the greater of hydrostatic pressure, slamming pressure, or slamming pressure at the forward end. The chapter allows the calculation of all types of pressure. The larger pressure for the bottom is the slamming pressure, and the larger for the sides is the hydrostatic pressure. There is a formula that gives the equivalent hydrostatic pressure for plating above the waterline. The slamming pressure is also given in Section 2, Formula C201:

$$P_{sl} = 1.3\, k_i \left(\frac{\Delta}{nA}\right)^{0.3} T_0^{0.7}\, \frac{50-\beta_x}{50-\beta_{cg}}\, a_{cg} \tag{4}$$

Where P_{sl} is the slamming pressure in kN/m², k_i is the longitudinal distribution factor, n is the number of hulls, A is the design load area for element considered, T_0 is the draught at L/2 in m at normal operation condition at service speed, Δ is the fully loaded displacement, β_x is the deadrise angle at transverse section considered and β_{cg} is the deadrise angle at CG.

Regarding the lateral loads on the hull, the regulations establish a formula for calculating slamming and hydrostatic pressure. However, hydrostatic pressure is higher than lateral slamming pressure. For load points above the waterline, there is an equation that gives a corresponding pressure on C501:

$$p = 10h_0 + \left(k_s - 1.5\frac{h_0}{T}\right) C_W \tag{5}$$

For load points below waterline:

$$p = ak_s + (C_W - 0.67h_0) \tag{6}$$

Where p is the sea pressure in kN/m², h_0 is the vertical distance in meters from the waterline, k_s is a longitudinal distribution factor given by the rules, T is the draft in meters, C_w is the wave coefficient calculated in other part of the rules.

Using the Eq. (4),(5) and (6) and the hydrodynamic and geometric parameters of the hull, the graphs shown in Fig. 5 were constructed. The graph in Fig. 5a shows the slamming pressure on the bottom of the hull along its length. It is clear that the highest pressures are found in the regions near the bow. The graph in Fig. 5b shows the hydrostatic pressures on the side of the vessel. Again, it can be seen that the highest pressures are found in the regions near the bow, even on the side of the vessel.

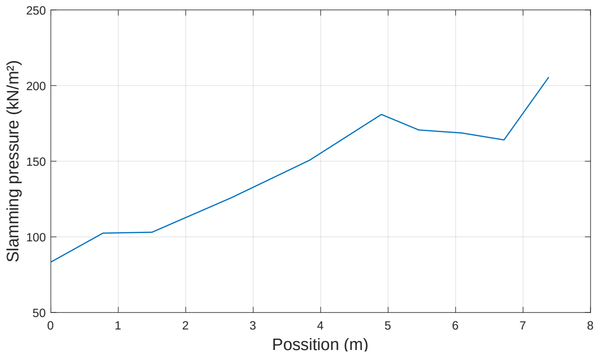

(a) Slamming pressure at the bottom.

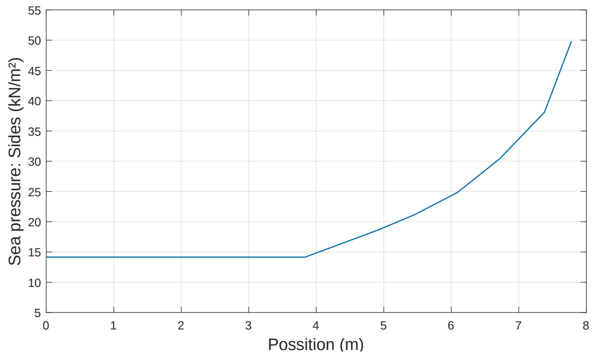

(b) Hydrostatic pressure at the sides.

Figure 5: Graphic of slamming and hydrostatic pressure.

5.4 Structural design

The maximum loads calculated for each part of the hull are then used to design the thicknesses of the panels, stiffeners and frames. Part 3, Chapter 4 of the DNV standard contains the design rules for laminates. According to criterion B502 in Section 5, the ultimate stress of the material must be 30% of the rupture stress for this type of structure, i.e. using the material properties in Table, the ultimate stress is 36.75 Mpa. To calculate the fracture stress, equation B502A from Section 6 is used:

$$\sigma = C_3 \cdot 1000\,\frac{b^2}{t^2}\,p \tag{7}$$

where σ is the ultimate tensile stress, t is the thickness in millimeters, b is the width of the structural hull panel varying along the length, p is the design local pressure calculated and C_3 is a factor that concerns the panel edge condition given by the rules.

Equation (7) can be manipulated to obtain the plate thickness using the ultimate stress previously calculated.

A sandwich laminate structure is used on the side of the hull. This structure provides a great structural advantage by increasing the moment of inertia of the panel without requiring a large increase in weight, making it more resistant and lighter. In Section 5 of the DNV rules, there is B201 equation for determining the stresses in sandwich laminates:

$$\sigma = \frac{160pb^2}{W}\,C_n C_1 \tag{8}$$

Where W is the section modulus, C_n and C_1 are factors regarding panel edge condition.

By rearranging Eq. (7) and using the ultimate stress, it is possible to determine the thickness of the walls of the sandwich laminate.

The last components to be designed are the transverse and longitudinal stiffeners. The longitudinal stiffeners have an inverted “U” shape and the transverse stiffeners have an “I” shape. The first step is to calculate the bending moments for panels subjected to pressure loads, as given in equation B201 in Part 3, Chapter 4, Section 7:

$$M = \frac{pbl^2}{c_1} \tag{9}$$

Where b is the load area, meaning the spacing between frames or stiffeners, l is the beam’s span and c_1 is a factor related to the analysis on the ends or mid-span of the beam.

The next step is to determine the required section modulus. The formula can be found under B601 in the same chapter. The allowable ultimate stress already calculated is used again. The section modulus Z is determined by:

$$Z = \frac{M}{\sigma} \tag{10}$$

With the determination of the section modulus and the use of a catalog of stiffiners, with their respective area moments of inertia, the selection of the most appropriate stiffiner for each section is automatic, and the smallest stiffiner can provide the calculated section modulus.

5.5 Design Variables

In order to perform the structural optimization of the hull, a standard floor plan must first be defined. The Fig. 6 shows the standard basic layout used, in which the bottom panels of the hull are made of fiberglass laminate, the side walls are made of fiberglass sandwich laminate and PVC foam, and longitudinal stiffeners of type "U" and stiffeners of type "I" are used in the transverse direction. It was decided to use 2 longitudinal stiffeners at a distance of 0.75 meters from each side of the hull. The design variables were defined as the distances between the transverse frames (highlighted in red in the Fig. 6), with a limit of up to 10 frames along the length of the hull.

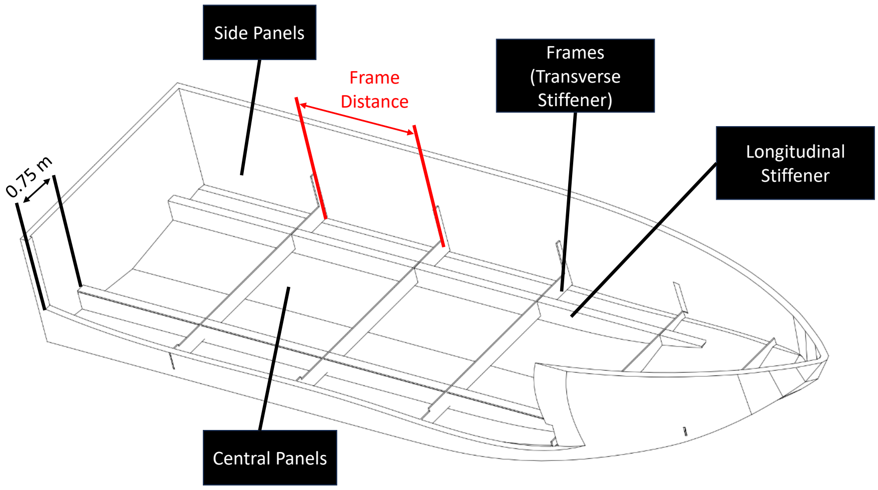

Figure 6: Hull structural layout.

6. RESULTS

Figure 7 shows the results of the structural masses obtained during the optimization. Here you can see the 5000 individuals analyzed. It is easy to see that around individual 500, the optimal value for the distances between the cavities was found, since the optimizer did not find ways to further reduce the mass of the hull.

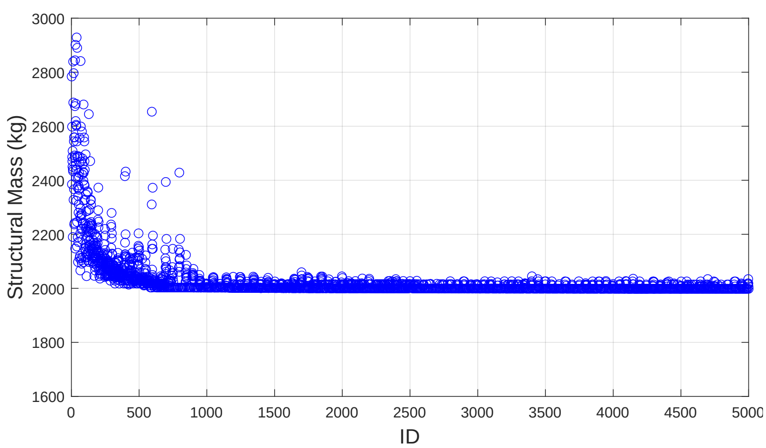

Figure 7: Mass reduction during optimization.

The optimal individual has a mass of 2006 kg, the Fig. 8a shows the thicknesses of the central panels along the length of the hull, and the Fig. 8b shows the thickness of the fiberglass on one side of the structural sandwich used in the manufacture of the lateral part of the hull. The Fig. 8 shows that the greatest thicknesses are found in the middle of the vessel, which is to be expected considering that this is the area where the greatest loads are found.

Figure 9a shows the dimensions of the longitudinal stiffeners. For the stiffeners, the use of a “U” type was considered, with the red line indicating the height dimensions and the blue line indicating the width of the stiffener for each section. The Fig. 9b shows the dimensions of the frame stiffeners, in this case was considered a type “I” stiffener.

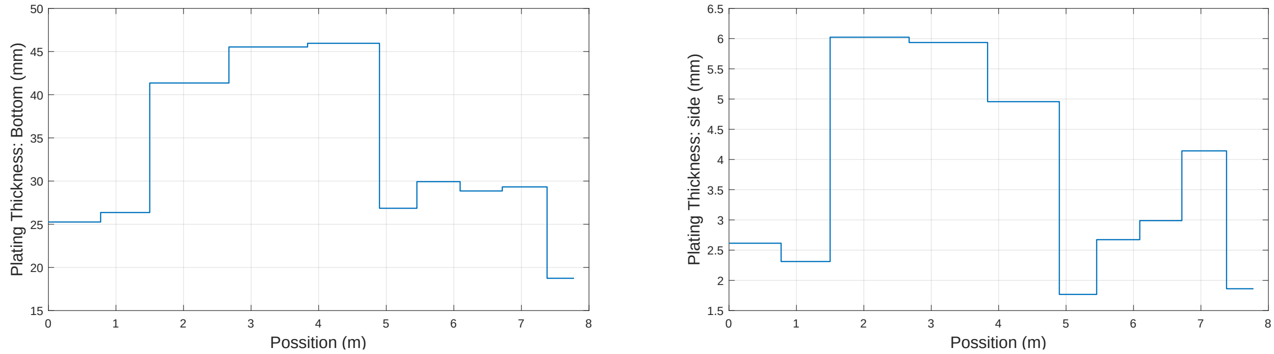

(a) Central panels of the bottom widt. (b) Plate thickness of one side of the sandwich.

Figure 8: Plate thickness along the length.

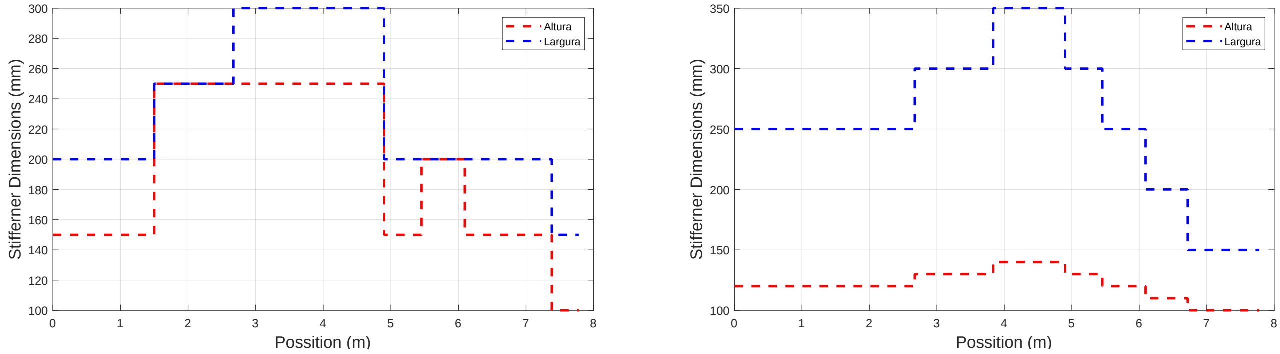

(a) (b) Frames.

Figure 9: dimensions of the stiffeners.

7. CONCLUSION

This paper presents a study on the structural optimization of a composite hull for a ground effect vehicle. The objective of the article was to consider the manufacturing processes commonly used in the marine industry and thus evaluate their applicability to this type of vehicle. The design method was carried out considering the criteria established by DNV. The thicknesses of panels, stiffeners and frames were designed and the optimization objective was to minimize the structural mass. The optimization results show that the structures found are capable of meeting all the criteria of the marine standards, thus ensuring the safety of the vehicle occupants.

On the other hand, the value of the found mass is quite high considering the type of designed vehicle, i.e., the use of marine manufacturing processes does not seem to be suitable for this type of vehicle. Therefore, for future work, it is recommended to evaluate aeronautical processes for the fabrication of the hull in order to estimate the gain in structural efficiency that they would bring to the hull.

8. REFERENCES

Amaral, J.R., 2016. “Engenharia naval”.

Badini, C., 2013. *Materiali compositi per l’ingegneria*. Strumenti per l’ingegneria. CELID. ISBN 9788876619922. URL `https://books.google.com.br/books?id=SXnplwEACAAJ`.

Budynas, R. and Nisbeth, J., 2016. *Elementos de Máquinas de Shigley - 10ª Edição*. McGraw Hill Brasil. ISBN 9788580555554. URL `https://books.google.com.br/books?id=ekN4CwAAQBAJ`.

Cardoso, A.A., 1994. *Síntese racional automatizada de Cavernas de Embarcações*. Master’s thesis, Universidade de São Paul, São Paulo.

Coelho, L.C., 2010. “Desafios logísticos na amazônia”. https://www.logisticadescomplicada.com/desafios-logisticos-na-amazonia/googlevignette.

Costanza, R., Groot, R., Sutton, P., Van der Ploeg, S., Anderson, S., Farber, S. and Turner, R., 2014. “Changes in the global value of ecosystem services”. *Global Environmental Change*, Vol. 26, p. 152–158. doi: 10.1016/j.gloenvcha.2014.04.002.

den Breejen, E., 2018. *Wing in ground vehicles operating as high-speed passenger ferries*. Master’s thesis, TUDelft.

DNV, 2012. “High speed, light craft and naval surface craft part 3 chapter 4”. DET NORSKE VERITAS, ehttps://www.dnv.com/. Accessed 16 jul 2023.

Halloran, M. and O’Meara, S., 1999. *Wing in Ground Effect Craft Review*, DSTO Aeronautical and Maritime Research Laboratory.

Jones, R., 1998. *Mechanics Of Composite Materials*. 500 Tips. Taylor & Francis. ISBN 9781560327127. URL `https://books.google.com.br/books?id=oMph2kNG3yAC`.

Kamarul, A.M., Xu, Y., Lewis, A. and Tiu, W., 2017. “A review on hull design for amphibian aircraft”. *Engineering Technology Research*, Vol. 1, p. 6.

Mathworks, 2018. “gamultiobj”. URL `https://www.mathworks.com/help/gads/gamultiobj.html`.

Nebylov, A., 2001. “Wing-in-ground flight automatic control principles, systems and application advantages”. *IFAC Proceedings Volumes*, Vol. 34, pp. 542–547. doi:10.1016/S1474-6670(17)40784-1.

Neto, F. and Pardini, L., 2006. *Compósitos estruturais: ciência e tecnologia*. Edgard Blücher. ISBN 9788521203971. URL `https://books.google.com.br/books?id=r`$_J4PgAACAAJ$.

Papadopoulos, C., Mitridis, D. and Yakinthos, K., 2022. “Conceptual design of a novel unmanned ground effect vehicle (ugev) and flow control integration study”. *Drones*, Vol. 6, p. 25. doi:10.3390/drones6010025.

Rayes, C.B. and Tancredi, T.P., 2013. “22nd international congress of mechanical engineering (cobem 2013)”. p. 13.

Reddy, J., 2003. *Mechanics of Laminated Composite Plates and Shells: Theory and Analysis, Second Edition*. Taylor & Francis. ISBN 9780849315923. URL `https://books.google.com.br/books?id=Wk-mmgEACAAJ`.

Rozhdestvensky, K., 2000. *Aerodynamics of a Lifting System in Extreme Ground Effect*, Springer International Publishing. ISBN 978-3-642-08556-7. doi:10.1007/978-3-662-04240-3-10.

Silva, A. and Cavalcante, M., 2016. “AvaliaÇÃo da resistÊncia de materiais compÓsitos reforÇados por fibras longas unidirecionais empregando modelos da micromecÂnica”.

Tsai, S.W. and Wu, E.M., 1971. “A general theory of strength for anisotropic materials”. *Journal of composite materials*, Vol. 5, No. 1, pp. 58–80.

Wiriadidjaja, S., Zhahir, A., Mohamad, Z., Razali, S., Puaat, A. and Ahmad, M., 2018. “Wing-in-ground-effect craft: A case study in aerodynamics”. *International Journal of Engineering and Technology(UAE)*, Vol. 7, pp. 5–9. doi: 10.14419/ijet.v7i4.13.21319.

Yun, L., Bliault, A. and Doo, J., 2010. *WIG craft and ekranoplan: Ground effect craft technology*. ISBN 978-1-4419-0041-8. doi:10.1007/978-1-4419-0042-5.

9. RESPONSIBILITY NOTICE

The following text, properly adapted to the number of authors, must be included in the last section of the paper: The authors are solely responsible for the printed material included in this paper.